

## Investigation of Coil Effect on the Crystalline Melting Transition in Liquid Crystalline Rod-Coil Oligomers by Raman Spectroscopy

Soo-Chang Yu\*, Keunok Han Yu, Jongwan Yu, and Myongsoo Lee<sup>†</sup>

Department of Chemistry, Kunsan National University, Kunsan, Chonbuk 573-701, Korea

<sup>†</sup>Department of Chemistry, Yonsei University, Sinchon 134, Seoul 120-749, Korea

Received March 25, 1998

### Introduction

Most rod-coil liquid crystalline oligomers have their own crystalline melting points, at which a dramatic change occurs in the intermolecular interactions between the neighboring mesogenic units.<sup>1-3</sup> For this class of molecules, the melting point of each derivative is largely affected by the coil length. The coil effect has been widely studied by the differential scanning calorimetry (DSC) experiments.<sup>4</sup> However, this technique is not amenable to the examination of the microstructural change during the variation of coil conformations. So, it is of our interest to investigate the mechanism in which the coil unit affects the crystalline phase transition by using Raman spectroscopy, which is very efficient in studying the microstructural change at the molecular level.

The Raman spectroscopic study has been successfully done on the salt or temperature dependent conformational change of the esterification product of ethyl 4-[4'-oxy-4-biphenylcarbonyloxy]-4'-biphenylcarboxylate with an oligomer having ethylene oxide units, abbreviated as oligomer I.<sup>5</sup> In these studies, the modifications of the Raman bands in both the relative intensity and the band frequency were observed during the crystalline phase transition. Based on the molecular structural information from the Raman mode analysis, it was demonstrated that the partial bond rotation around the ketone linkage of the aryl C-C(=O)O is closely related to the breaking of the intermolecular interactions between the neighboring mesogens. It is noteworthy that the increase of the LiCF<sub>3</sub>SO<sub>3</sub> concentration in oligomer I weakens the intermolecular forces, which leads to the Raman result very similar to that of the temperature dependent experiment.

In this report, we extend the temperature and salt dependent Raman study to a new model compound, the esterification product of docosyl 4-[4'-oxy-4-biphenylcarbonyloxy]-4'-biphenylcarboxylate with ethylene oxide units, abbreviated as oligomer II, which is an analogous molecule of oligomer I, but with a long alkyl chain in the coil unit instead of ethyl group for oligomer I. By comparing the Raman results on these two molecules, we propose that the crystalline phase transitions of the rod-coil oligomers are promoted by both the breaking of the intermolecular interactions and the conformational rearrangement of the coil unit, which is thought to occur in a concerted mechanism.

### Experimental

The following molecules are the model compounds of

this study. The synthesis of oligomer I was reported in the previous literature.<sup>6,7</sup> Oligomer II was synthesized based on the procedure for oligomer I with some minor modifications.

CH<sub>3</sub>O-(CH<sub>2</sub>CH<sub>2</sub>O)<sub>12</sub>-C<sub>6</sub>H<sub>4</sub>C<sub>6</sub>H<sub>4</sub>COO-C<sub>6</sub>H<sub>4</sub>C<sub>6</sub>H<sub>4</sub>COO-CH<sub>2</sub>CH<sub>3</sub>  
: oligomer I

CH<sub>3</sub>O-(CH<sub>2</sub>CH<sub>2</sub>O)<sub>12</sub>-C<sub>6</sub>H<sub>4</sub>C<sub>6</sub>H<sub>4</sub>COO-C<sub>6</sub>H<sub>4</sub>C<sub>6</sub>H<sub>4</sub>COO-(CH<sub>2</sub>)<sub>21</sub>-CH<sub>3</sub>  
: oligomer II

The Renishaw Raman micro system 2000 was used to get Raman spectra.<sup>8</sup> As an excitation source, the 632.8 nm with a maximum power of 25 mW from Spectra Physics Model 127-75RP HeNe laser was used. The laser power at the sample was *ca.* 5 mW and the spectra were recorded for between 20-50 scans depending on the samples. The resolutions of all the spectra are within  $\pm 2$  cm<sup>-1</sup>. All the samples were put on glass slides, and data were acquired by using an Olympus 20x ultra long working distance objective lens. For the temperature control, the Linkam heating and freezing stage (THMSE 600) and controller (TMS 92) were used. The samples were heated at 10 °C/min and left for 5 min for equilibrium before collecting data. All the spectra were manipulated with the software provided by Renishaw, and background corrections were made when needed.

### Results and Discussion

**Temperature Dependent Study.** The temperature dependent modification of the mesogenic modes is ascribed to the change in the intermolecular interactions between the neighboring mesogenic units. Yu *et al.*<sup>5</sup> proposed that the intermolecular interactions start to be gradually weakened at the beginning stage upon either stepwise addition of salts or temperature increase, leading to the relaxation of the steric strain around the aryl C-C(=O)O. This process is expected to continue until most of the interactions are finally broken down to invoke the dramatic conformational change at the crystalline melting point.

Figure 1 shows the temperature dependent Raman spectra of oligomer I and oligomer II, both of which are normalized with respect to the strongest peak in the range 1250-1300 cm<sup>-1</sup>. Compared with oligomer I, the Raman spectral profile of oligomer II shows the additional bands at 1118, 1132, 1205, and 1295 cm<sup>-1</sup>, all of which are assigned to vibrational modes of the alkyl chain.<sup>9</sup> These alkyl bands gradually decrease in the relative intensity as the temperature increases until they almost become extinct above the crystalline melting temperature.

The Raman bands in the range 1150-1300 cm<sup>-1</sup> show the characteristic features of the conformational variation of the mesogenic units.<sup>5</sup> The 1173 and 1189 cm<sup>-1</sup> bands of both

\*Author to whom correspondence should be addressed.

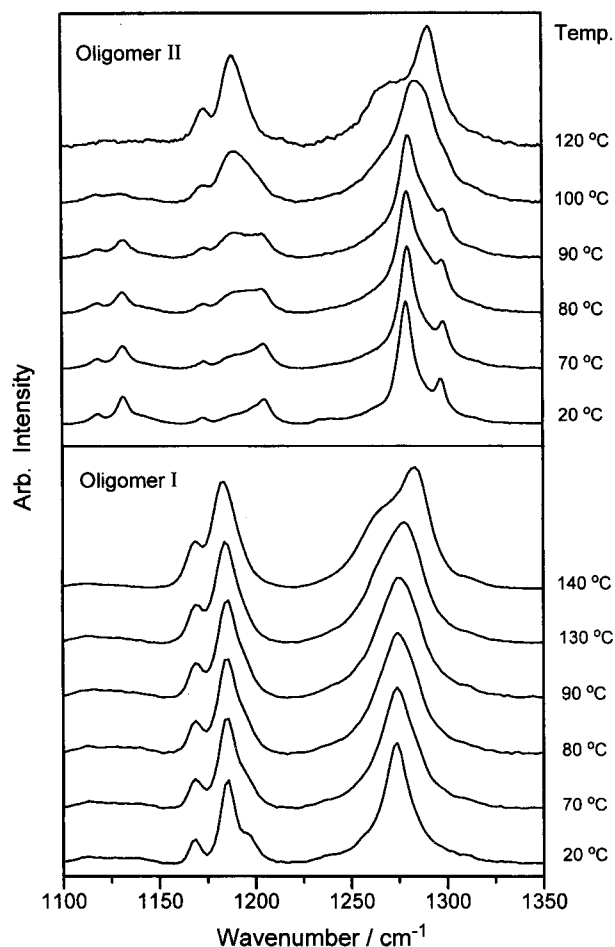


**Figure 1.** The evolution of the Raman bands ( $1100\text{--}1350\text{ cm}^{-1}$ ) as a function of temperature for oligomer II (top), and oligomer I (bottom).

oligomer I and oligomer II are assigned to the aryl C-H in-plane modes,<sup>9</sup> and both molecules show spectral changes in a very similar pattern upon temperature increase. This behavior is also found both in the  $1270\text{ cm}^{-1}$  mode of oligomer I and the  $1279\text{ cm}^{-1}$  mode of oligomer II, which are assigned to the combination modes of the aryl C-C(=O)O and C-H in-plane vibrations.

The crystalline melting points measured by DSC are  $134\text{ }^{\circ}\text{C}$  and  $98\text{ }^{\circ}\text{C}$  for oligomer I and oligomer II, respectively. Even though the Raman spectra of these two molecules show a noticeable difference below the melting temperatures, their mesogenic modes show almost the same Raman spectral feature above the melting temperatures. This result suggests that the lowering of the crystalline melting point for oligomer II with respect to oligomer I is mainly attributed to the weakening of intermolecular interactions such as van der Waals interaction, dipole-dipole interaction, and hydrogen bonding, due to the loosening of the packing between the mesogenic units.

The above argument can be further verified by the observation of carbonyl mode which is susceptible to hydrogen bonding. When the intermolecular hydrogen bond is formed, the mesogenic units around the carbonyl group will accordingly become more tightly packed together.<sup>10</sup> The comparison of the Raman spectral shape for oligomer I with

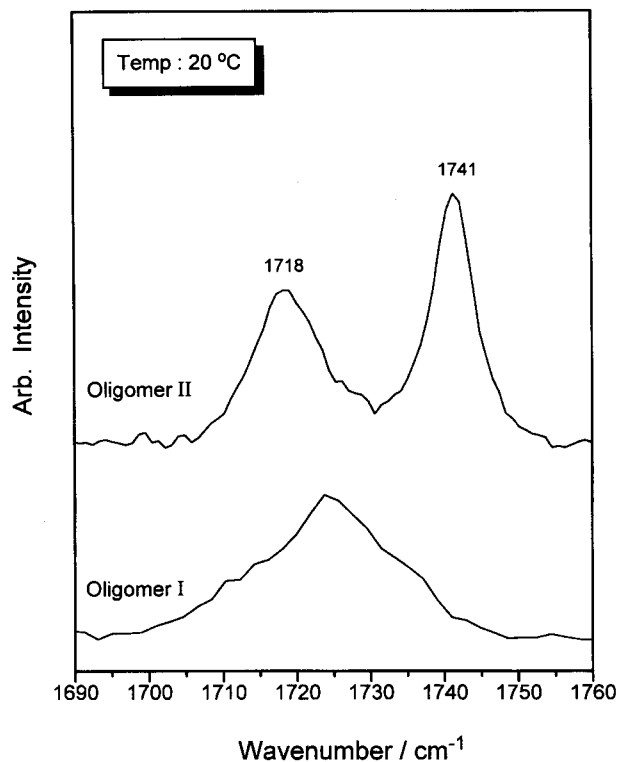


**Figure 2.** The carbonyl stretching modes for oligomer II (top) and oligomer I (bottom). The multiplex maxima for oligomer I are due to the formation of hydrogen bonding with the neighboring aryl hydrogen.

that of oligomer II at room temperature underlines this hypothesis by showing that the loosely packed oligomer II has the well-separated two C=O Raman bands instead of a single blunt band for oligomer I (Figure 2). For oligomer II, the lower frequency mode at  $1718\text{ cm}^{-1}$  is assigned to the C=O moiety located between the two biphenyl groups and the higher frequency mode at  $1741\text{ cm}^{-1}$  represents the vibrational mode of the terminal C=O, whose hydrogen bond formation is hampered by the attached long alkyl chain. Meanwhile, for oligomer I, the two Raman bands are merged into a broad band since the higher frequency mode shifts downward as the hydrogen bond is formed. This result provides a strong evidence for the lowering of crystalline melting point by attaching a long alkyl chain in the coil unit; the long alkyl chain exerts the steric hindrance effect on a neighboring molecule, so that the intermolecular interactions are significantly weakened in oligomer II.

**Salt Dependent Study.** The mesogenic Raman bands undergo significant changes upon the addition of  $\text{LiCF}_3\text{SO}_3$  (Figure 3). As the salt concentration is increased above a certain level in the liquid crystalline matrix, some of the salts are bound to the ether oxygens and the others remain undissociated. For oligomer I, the undissociated salts are interspersed in the mesogen matrix, resulting in the conformational change around the aryl C-C(=O)O by weakening the intermolecular interactions.<sup>5</sup> For oligomer II, however, the addition of salt does not change the Raman result as much as that of oligomer I; the spectral progression of the mesogenic unit of oligomer II at  $[\text{Li}^+]/[\text{EO}] = 0.6$ , where [EO] represents the concentration of ethylene ox-

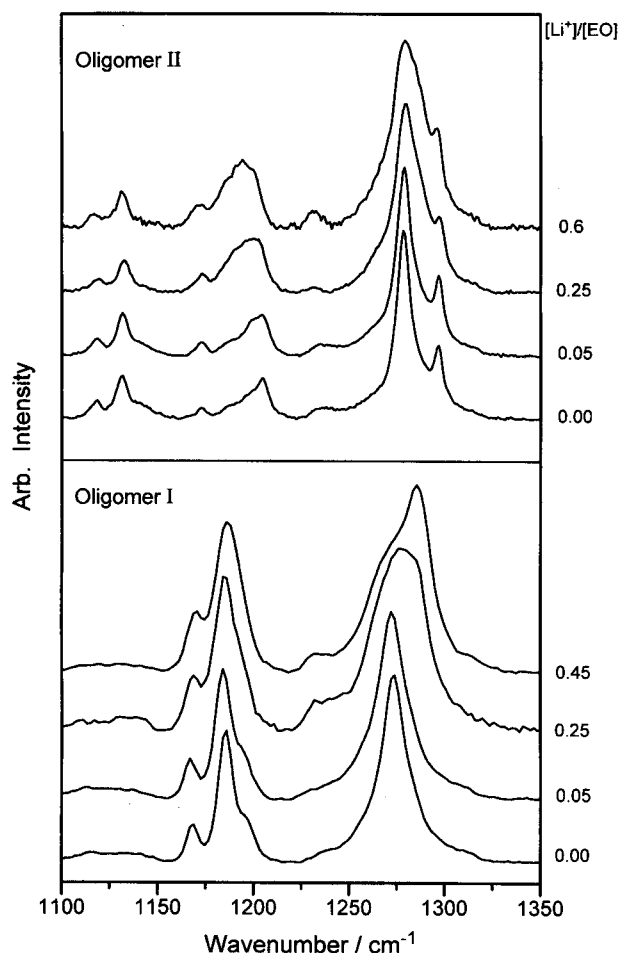


**Figure 3.** The evolution of the Raman bands ( $1100\text{--}1350\text{ cm}^{-1}$ ) as a function of salt concentration for oligomer II (top), and oligomer I (bottom).  $[\text{Li}^+]/[\text{EO}]$  represents the mole ratio of the  $\text{LiCF}_3\text{SO}_3$  to the ethylene oxide unit. All the spectra were acquired at room temperature ( $20\text{ }^\circ\text{C}$ ).

ide units, is significantly less developed than that of oligomer I at  $[\text{Li}^+]/[\text{EO}]=0.4$ , although the amount of salt exceeds by 50% for the former.

Comparison between the variations of the spectral profiles by the salt addition and the temperature change gives us an insight into the molecular structure based interpretation of the intercalation effect of the added salts. For oligomer I, the band shapes of the mesogenic modes change with the salt concentration and finally becomes similar to those of the salt-free oligomer I at high temperature. However, for oligomer II, the room temperature band shape at  $[\text{Li}^+]/[\text{EO}]=0.6$  is noticeably different from that of the salt-free one measured above the crystalline melting temperature.

This result gives us an unambiguous evidence for the interpretation of the phase transition phenomena in terms of both the degree of packing among the mesogenic units induced by the intermolecular interactions and the conformational change induced by the attached coil unit. In oligomer I, the packing is so tight that the spacing is thought to be very narrow. As a result, the effect of the salt concentration is so great that even a small concentration increase can largely alter the interactions. In contrast, for oligomer II, the long alkyl chain makes the packing so loose

that the neighboring molecules are spaced wide enough to accommodate free space for the undissociated salts, which explains why it is hardly affected by the salt addition.

The phase transition is thought to occur *via* the rotation about the single bond between the phenyl rings, with the carbonyl group positioned parallel to the adjacent phenyl ring<sup>11</sup> or via the rotation about the ketone linkage of the aryl  $\text{C}\text{--}\text{C}(=\text{O})\text{O}$ ,<sup>2,5,12</sup> both of which should be assisted by the concerted conformational change of the coil unit. In oligomer I, the phase transition is induced mainly by the breaking of the intermolecular interactions, which is immediately followed by the conformational change in the mesogenic unit, since the short ethylene oxide coil unit feels only minor steric strain during the conformational change. This explains why oligomer I can undergo phase transition by the salt induced weakening of the intermolecular forces even at room temperature. In oligomer II, however, the phase transition is dominated by the conformational change of the coil unit, during which it must overcome the steric strain induced by the long alkyl chain. Therefore, its crystalline melting process needs large amount of thermal energy even though the intermolecular forces of oligomer II are much weaker than that of oligomer I.

### Conclusion

The Raman spectroscopic studies were done for rod-coil oligomers to investigate the coil effect on the crystalline melting transitions. This Raman study presents two limiting cases among rod-coil oligomers where the crystalline melting process is dominated by either the breaking of intermolecular interactions or the conformational rearrangement of the coil unit. Oligomer I represents the former case because its short coil unit facilitates the tight packing to provide the strong intermolecular interactions, while the conformational rearrangement of the coil unit can take place easily once the intermolecular forces are broken by either the salt addition or temperature increase. Meanwhile, oligomer II represents the latter case because its long alkyl chain prevents the intermolecular interactions and the crystalline melting is dominated by the conformational change of the coil unit which is expected to assist in the rotation about the chemical bond in the mesogenic unit. Considering the Raman results, both of these two dynamical processes seem to be responsible for the phase transition of rod-coil type oligomers in a concerted mechanism. Even though the stationary state Raman technique cannot provide the direct experimental evidence for the molecular dynamical information on a real time scale, the temperature-jump laser technique<sup>13</sup> is expected to be a very strong candidate to verify the proposed two-step dynamics derived from our current Raman study.

**Acknowledgment.** The present studies were supported by the Basic Science Research Institute Program, Ministry of Education, 1997, Project No. BSRI 97-3431

### References

1. Ellis, G.; Marco, C.; del Pino, J.; Lorente, J.; Gomez, M. A.; Fatou, J. G. *Vib. Spectrosc.* **1995**, *9*, 49.
2. Jedlinski, Z.; Franek, J.; Kulezyeki, A.; Sirigu, A.;

- Carfagna, C. *Macromolecules* **1989**, 22, 1600.
- del Pino, J.; Gomez, M. A.; Ellis, G.; Marco, C.; Fatou, J. G. *Macromol. Chem. Phys.* **1994**, 195, 2049.
  - Bahadur, B. *Liquid Crystals: Applications and Uses*; World Scientific Publishing Co. Singapore, 1990.
  - Yu, S.-C.; Paek, J.; Yu, K. H.; Ko, S. B.; Cho, I.-H.; Lee, M. *Bull. Korean Chem. Soc.* **1997**, 18, 773.
  - Lee, M.; Oh, N.-K.; Lee, H. K.; Zin, W. C. *Macromolecules* **1996**, 29, 5567.
  - Lee, M.; Oh, N.-K. *J. Mater. Chem.* **1996**, 6, 1079.
  - Williams, K. P. J.; Pitt, G. D.; Smith, B. J. E.; Whitley, A.; Batchelder, D. N.; Hayward, I. P. *J. Raman Spectrosc.* **1994**, 25, 131.
  - Yu, S.-C.; Chung, D.; Yu, K. H.; Kim, D. H.; Oh, N. K.; Lee, M.; Ko, S. B.; Cho, I. H. *Bull. Korean Chem. Soc.* **1996**, 17, 1004.
  - Wu, P. P.; Hsu, S. L.; Thomas, O.; Blumstein, A. *Polymer Physics* **1986**, 24, 827.
  - del Pino, J.; Gomez, M. A.; Marco, C.; Ellis, G.; Fatou, J. G. *Macromolecules* **1992**, 25, 4642.
  - Shilov, S.; Volchek, B.; Zuev, V.; Skorokhodov, S. *Macromol. Chem. Phys.* **1994**, 195, 865.
  - Thompson, P. A.; Eaton, W. A.; Hofrichter, J. *Biochemistry* **1997**, 36, 9200.

## FT-IR Spectral Analysis of Self-Assembled Monolayer Film of *N*-(2-Mercaptoethyl)-Anthraquinone-2-Amide on Gold

Sang Jung Ahn and Kwan Kim\*

Department of Chemistry and Center for Molecular Catalysis, Seoul National University, Seoul 151-742, Korea  
Received May 4, 1998

### Introduction

Redox molecules adsorbed on metal substrates have been regarded to be model systems to understand electron transfer in biological systems.<sup>1</sup> From the fact that quinone derivatives play important roles in biological systems,<sup>2</sup> their redox properties as well as their adsorption behavior on various electrode surfaces have been studied using electrochemical and spectroscopic techniques.<sup>3-5</sup>

The most popular quinoids compounds naturally occurring are anthraquinone derivatives.<sup>6</sup> In a hope eventually to prepare electroactive devices that could be applied as a biosensor, we are currently interested in the adsorption behavior of various anthraquinone derivatives on noble metals such as gold and silver. Recently, we found that a planar molecule, *i.e.*, anthraquinone-2-carboxylic acid, could be self-assembled and close-packed on a silver surface, forming a brick-like architecture.<sup>7</sup> On the other hand, in a molecular dynamics simulation study on benzylthiolate on Au (111),<sup>8</sup> it was found that the methylene group situated at between the sulfur head group and the benzene ring moiety should play a key role for the adsorbate molecules to arrange in a herringbone type structure.<sup>9</sup> On these grounds, we have investigated the adsorption behavior of *N*-(2-mercaptoethyl)-anthraquinone-2-amide, a flexible nonplanar anthraquinone derivative, on a gold surface, and herein we hope briefly to discuss its orientation on gold that could be deduced from the FT-IR spectroscopic data.

### Experimental

*N*-(2-mercaptoethyl)-anthraquinone-2-amide (AQ-CONH-

C2-SH) was synthesized by coupling 2-aminoethanethiol with anthraquinone-2-carboxylic acid. The product was confirmed from H-NMR, IR, and mass spectra. Unless otherwise specified, all chemicals and gases were reagent grade and used as received.

Gold substrates were prepared by resistive evaporation of titanium (Aldrich, 99.99%) and gold (Aldrich, 99.99%) below  $10^{-6}$  Torr on a batch of glass slides, cleaned previously with a hot piranha solution (30%  $\text{H}_2\text{O}_2$ : $\text{H}_2\text{SO}_4$ =1:4) and then sonicated in deionized water. After deposition of approximately 300 nm of gold, the evaporation chamber was backfilled with nitrogen.

Adsorbate solutions were prepared by dissolving weighed portions of AQ-CONH-C2-SH in nitrogen-bubbled anisole to desired concentrations covering the range from  $10^{-3}$  to  $10^{-7}$  M. Precleaned glass vials were used as the self-assembly cells. The gold substrates were immersed subsequently into the adsorbate solutions for a predetermined period of time. After the substrates were removed, they were rinsed with excess ethanol and then subjected to a strong nitrogen gas jet to blow off any remaining liquid droplets on the surface or the edges of the substrates.

The infrared spectra were obtained with a Bruker IFS 113v Fourier transform spectrometer equipped with a Globar light source and a liquid  $\text{N}_2$ -cooled mercury cadmium telluride detector. The method for obtaining the reflection-absorption infrared (RAIR) spectra has been reported previously.<sup>10,11</sup> Each RAIR spectrum was obtained by averaging 1024 interferograms at  $4\text{ cm}^{-1}$  resolution, with *p*-polarized light incident on the gold substrate at  $80^\circ$ . The Happ-Genzel apodization function was used in Fourier transforming the interferograms. The RAIR spectra are reported as  $-\log(R/R_0)$ , where *R* and *R*<sub>0</sub> are the reflectivities of the sample and the bare clean metal substrates, respec-

\*Author to whom correspondence should be addressed.